



Research article

MEG3 sponges miRNA-376a and YBX1 to regulate angiogenesis in ovarian cancer endothelial cells

Yize Li^{a,1}, Lingling Zhang^{b,1}, Yongmei Zhao^c, Hongyan Peng^d, Nan Zhang^{e,**},
Wendong Bai^{c,*}

^a Departments of Clinical Oncology, Xijing Hospital, Fourth Military Medical University, Xi'an, Shaanxi, 710032, China

^b Departments of Blood Transfusion, Xijing Hospital, Fourth Military Medical University, Xi'an, Shaanxi, 710032, China

^c Department of Hematology, Xinjiang Command General Hospital of Chinese People's Liberation Army, Urumqi, 830000, Xinjiang, China

^d Department of Internal Medicine, 63650 Military Hospital, Urumqi, 830000, Xinjiang, China

^e Department of Dermatology, Xinjiang Command General Hospital of Chinese People's Liberation Army, Urumqi, 830000, Xinjiang, China

ARTICLE INFO

Keywords:

MEG3
Tube formation
Ovarian cancer
Endothelial cells
miR-376a
YBX1
RASA1
ODMECs
LncRNAs

ABSTRACT

Objectives: Recent studies have demonstrated maternally expressed gene 3 (MEG3) as a tumor suppressor across multiple malignancies. Meanwhile, the role of MEG3 in ovarian cancer needs further investigation. We aim to study the effects of MEG3 on angiogenesis in ovarian cancer and the underlying mechanisms.

Methods: The transcript levels of MEG3 in ovarian cancer samples from the GEPIA database were analyzed and compared to those in normal samples. The effect of MEG3 on the tube formation ability was quantified in ovarian carcinoma-derived microvascular endothelial cells (ODMECs). Through sequence analysis, we identified miR-376a as a major candidate to bind to MEG3. A MEG3-miR-376a binding site was identified via genetic modulation methods. RAS p21 protein activator 1 (RASA1) was screened as a middle player to bridge the role of miR-376a and angiogenesis. The regulation between miR-376a and RASA1 was confirmed via a dual-luciferase reporter assay. Finally, the competition was explored between Y-box binding protein 1 (YBX1) and miR-376a in binding to MEG3.

Results: MEG3 was significantly downregulated in ODMECs compared with normal ovarian endothelial cells. Overexpression of MEG3 led to reduced tube formation of ODMECs. The MS2 hairpin assay showed that MEG3 acted as a platform to sponge miR-376a. RASA1, a key suppressor of tube formation, was directly targeted by miR-376a. Further, MEG3 suppressed angiogenesis through the miR-376a/RASA1 axis in ODMECs. Finally, YBX1 and miR-376a were competitively bound to MEG3.

Conclusion: This study uncovered a novel mechanism that MEG3 sponged miRNA-376a and YBX1 to regulate the expression of RASA1 and exert an effect on the angiogenesis of ovarian cancer.

* Corresponding author.

** Corresponding author.

E-mail addresses: zhangnan424@sina.com (N. Zhang), bwddcgz@fmmu.edu.cn (W. Bai).

¹ These authors have contributed equally to this work: Yize Li, Lingling Zhang.

<https://doi.org/10.1016/j.heliyon.2023.e13204>

Received 5 June 2022; Received in revised form 10 January 2023; Accepted 19 January 2023

Available online 24 January 2023

2405-8440/© 2023 Published by Elsevier Ltd.

This is an open access article under the CC BY-NC-ND license

(<http://creativecommons.org/licenses/by-nc-nd/4.0/>).

1. Introduction

Ovarian cancer, the most lethal gynecological malignancy, is ranked as one of the top causes of cancer-related deaths among women in developed countries [1]. New blood vessel formation is critical to cancer growth and metastasis. Ovarian carcinoma-derived microvascular endothelial cells (ODMECs) are primarily responsible for blood vessel growth [2]. Therefore, novel therapeutics with anti-angiogenic effects achieved by targeting ODMECs would hold considerable potential for ovarian cancer treatment.

Maternally expressed gene 3 (MEG3), despite limited expression in various tumors, functions as a tumor suppressor gene in ovarian cancer [3]. Although the roles of MEG3 in the context of other cancers have been reported earlier [4], the effects of MEG3 in ODMECs have not been well elucidated. Long noncoding RNAs (lncRNAs) are at least 200 nt transcripts lacking protein-coding potential. Their roles have been recently appreciated in cancer diseases [5]. Recent research revealed that RNA-binding proteins (RBPs) and miRNAs control the post-transcription process, including RNA decay and stability, and regulate gene expression [6]. The roles of lncRNAs remain to be further investigated.

Here, we investigated MEG3 as a tumor suppressor in ODMECs and identified its interaction with miRNAs and RBPs. Through a luciferase reporter system in combination with bioinformatics analysis, MEG3 was shown to sponge miR-376a and modulate the transcript and protein levels of RASA1, leading to the modulation of tube formation in ODMECs. Our further experiments showed that YBX1, a nucleic acid binding protein, is bound to MEG3 through a conserved prediction motif. Our results indicated that YBX1 and miR-376a competitively sponge the tumor suppressor gene MEG3, thereby influencing tube formation by ODMECs.

2. Materials and methods

2.1. Samples collection and cell culture

Cancer tissue samples were collected from 14 patients histologically diagnosed with epithelial ovarian cancer in Xijing Hospital, per the protocol (registration number: KY20173063-1) approved by the Ethics Committee of Xijing Hospital, The Fourth Military Medical University. After resection, each tissue specimen was immediately portioned into three pieces for RNA analysis, protein extraction, and liquid nitrogen storage for further uses. Primary human ODMECs were isolated from tissues and cultured in EGM-2MV medium (#CC-3156, Lonza Group Ltd, Basel, Switzerland) with 10% FBS, 1% penicillin and streptomycin [7]. Cells were maintained in a humidified incubator at 5% CO₂, 37 °C.

2.2. Bioinformatics analysis

The transcript levels of MEG3 in ovarian cancer were calculated with the Gene Expression Profiling Interactive Analysis (GEPIA) (<http://gepia.cancer-pku.cn/>) [8]. The correlation between the clinical outcome of overall survival (OS) and MEG3 expression was analyzed with Kaplan–Meier Plotter (<http://kmplot.com/analysis/index.php?p=service&cancer=ovar>) [9]. The target genes for miRNAs were predicted with TargetScan (http://www.targetscan.org/vert_72/) [10]. The gene binding sites for miRNAs were predicted via Starbase (<http://starbase.sysu.edu.cn/starbase2/>) [11]. The protein-binding motifs in MEG3 were analyzed with the online platform RBPMap (<http://rbpmap.technion.ac.il/>) [12].

2.3. MS2 pulldown assay

MEG3, MEG3-MS2 and MEG3-mut-MS2 plasmids were first transfected into ODMECs, according to a previous study [13]. For MS2 pulldown assay, ODMECs were collected at 48 h post-transfection. Then ODMECs lysates were incubated with MBP-MCP-coated amylose resin (prepared at 4 °C) for 8 h. After incubation, the samples were extensively washed. Then 100 µl of buffer (containing 20 mM maltose) was used to elute bound MEG3-MS2 complexes. Eluted complexes were then analyzed by Western blotting to identify MEG3-associated proteins. We used quantitative reverse transcription polymerase chain reaction (qRT-PCR) analysis to identify any miRNA associated with MEG3.

2.4. Plasmid construction

GenePharma (Shanghai, China) constructed the sequences for MEG3, MEG3 mutant, RASA1 3' untranslated region (UTR, with miR-376a-binding site), and mutated RASA1 3' UTR. MEG3-expressing plasmids were constructed and cloned into a pCDNA3.0 and pGL3 vector. A six-repeat MS2 hairpin structure was then constructed and introduced into the pC3-MEG3 plasmid [14]. miR-376a site-directed mutagenesis for the MEG3 sequence was cloned in two parts: MEG3 mut-part1 with primers P1 5'-AGCCCCTAGCGCAGACGGCGGA-3' and P2 5'-AAAGTACAGTATCTCTCTTTGTA-3', MEG3 mut-part2 with primers P3 5'-TGCTCATACAAAGAGATACTGT-3' and P4 5'-TTTTTGTAAAGACAGGAAACACATT-3'. Then the primers P1 and P4 were used to amplify whole MEG3 mutation sequence in the recombinant products MEG3 mut-part 1 and mut-part 2. Plasmid construction was verified by sequencing before transfection. The MEG3 sequence was cloned into the pLenti-6.3 vector (Invitrogen, Carlsbad, CA, USA), and then ODMECs were transfected as previously described [15].

2.5. siRNA transfection and dual luciferase reporter assay

siRNAs were constructed by GenePharma (Shanghai, China). Transfection was done with the use of lipofectamine 2000 (Invitrogen). After transfection for 48 h, ODMECs were collected for downstream experiments. For the dual luciferase reporter assay, ODMECs were co-transfected with wildtype (WT)-RASA1-UTR or mutant (Mut)-RASA1-UTR, pRL-TK, and miRNA mimic. The dual luciferase activity was measured after transfection as previously described [16].

2.6. RNA immunoprecipitation (RIP)

ODMECs were first transfected with plasmid or mimic. With recombinant protein G agarose (Thermo Scientific, MA, US) to preclear the lysates, Cells (50 million in total) were separated into nuclear and cytoplasmic fractions. A small amount of the sample (1%) was taken as input. The left sample was incubated with anti-YBX1 antibodies or rabbit serum IgG. The samples were then treated with proteinase K. The mRNA or miRNA levels were analyzed by qRT-PCR as described previously [17].

2.7. qRT-PCR (quantitative reverse transcriptase PCR)

RNA isolation from ODMECs and reverse transcription for gene expression analysis were performed using PrimeScript™ RT Master Mix kit (TaKaRa, Japan). Reverse transcription for miRNA expression analysis was done with miScript Reverse Transcription Kit (Qiagen, Germany). The primers for qPCR were as follows: MEG3, forward 5'-TCCATGCTGAGCTGCTGCCAAG-3', reverse 5'-AGTCGACAAAGACTGACACCC-3'; PRKCE, forward 5'-CGAGGCCGTGAGCTTGAAG-3', reverse 5'-GCAATGTAGGGTTCGAGAAGG-3'; DOK1, forward 5'-CAATTCTGGGTAACGGTGCAG-3', reverse 5'-CCACCCTCAGCAGGTAGGA-3'; FGFR1, forward 5'-CCCGTAGCTCCATATTGGACA-3', reverse 5'-TTTGCCATTTTCAACCAGCG-3'; PRKD1, forward 5'-AGATGGCTTGCTCCATTGTGC-3', reverse 5'-GTCATGGCGAAAAAGCAGGAT-3'; HIF1A, forward 5'-GAAGTCGAAAAAGAAAGTCTCG-3', reverse 5'-CCTTATCAAGATGCGAACTACA-3'; PIK3CB, forward 5'-TATTGGACTTTGCGACAAGACT-3', reverse 5'-TCGAAGTACTGGTCTGGATAG-3'; WNT2B, forward 5'-GGGGCACGAGTGATCTGTG-3', reverse 5'-GCATGATGTCTGGGTAACGCT-3'; RASA1, forward 5'-ACTTGACA-GAAGCATAGCAGAAG-3', reverse 5'-GCCTCCGATCACTCTCTTA-3'; miR-5195-3p, forward 5'-ATCCAGTTCTCTGAGGGGGCT-3'; miR-3150a-3p (miR-3150), forward, 5'-CTGGGGAGATCCTCGAGGTTGG-3'; miR-361-5p (miR-361), forward, 5'-TTATCA-GAATCTCCAGGGGTAC-3'; miR-665, forward, 5'-ACCAGGAGGCTGAGGCCCT-3'; miR-376a-3p (miR-376a), forward, 5'-

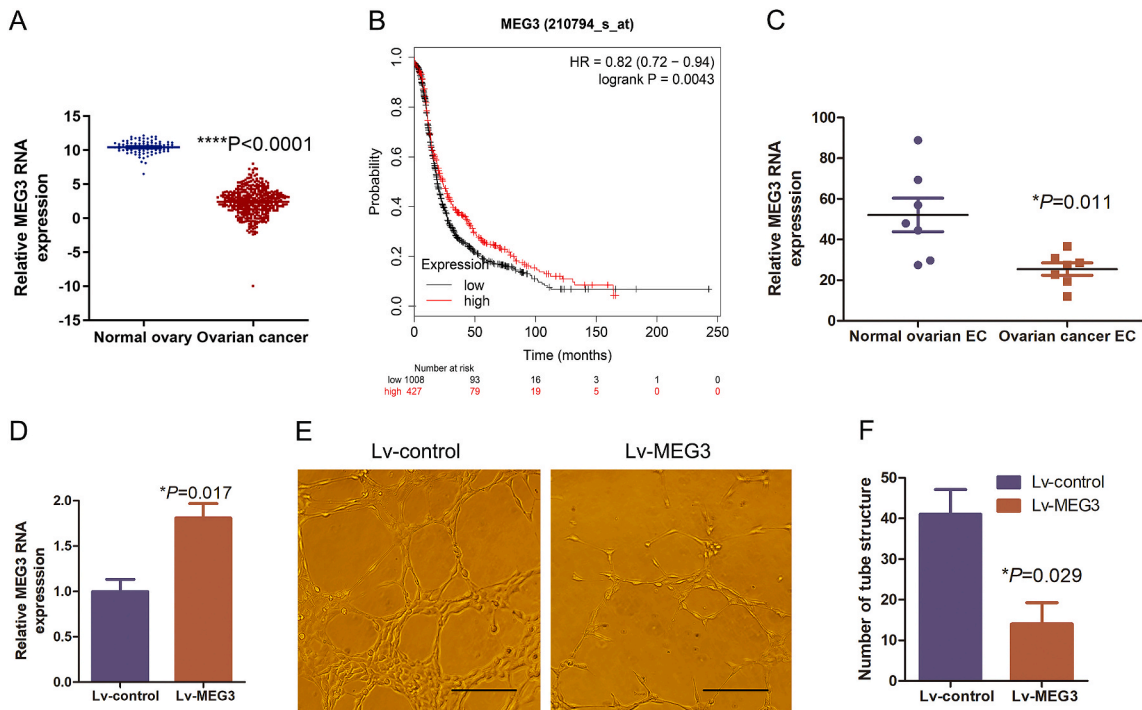


Fig. 1. MEG3 expression is downregulated in ODMECs, and overexpression of MEG3 inhibits tube formation by ODMECs. (A) MEG3 RNA levels in ovarian cancer and normal tissues based on the GEPIA database. (B) Kaplan-Meier analysis on overall survival rates based on MEG3 expression levels in 1435 patients with ovarian cancer. The mean value of MEG3 mRNA levels was applied to stratified patients into two groups. Log-rank test was applied to analyze the differences between the two groups. (C) Expression of MEG3 in ODMECs and normal ovarian microvascular endothelial cells. (D) qRT-PCR detection of lentivirus-mediated expression of MEG3 in ODMECs. (E) Analysis of tube formation by ODMECs infected with Lv-control or Lv-MEG3. Scale bar = 100 μm. (F) Quantified data from E.

ATCATAGAGGAAAATCCACGT-3'; and miR-485-5p, forward, 5'-AGAGGCTGGCCGTGATGAATTC-3'; reverse, Universal Primer (QIAGEN, Germantown, MD, USA).

2.8. Western blotting

Primary human ODMECs were lysed in ice-cold radioimmunoprecipitation assay buffer (RIPA; 20 mM Tris-HCl pH 7.4, 137 mM NaCl, 10% glycerol, 1% Triton X-100, 0.5% sodium deoxycholate, 0.1% SDS, 2 mM EDTA pH 8, 2 mM vanadate, 1 mM PMSF and a cocktail of protease inhibitors). The cell lysate was cleared by centrifugation, and an appropriate sample buffer was added. Samples were subjected to SDS-PAGE and immunoblotted using primary rabbit polyclonal anti-YBX1 (#ab76149; Abcam, Cambridge, UK), anti-RASA1 (#ab40677; Abcam), and mouse monoclonal anti-β-actin (#A5441, Sigma-Aldrich) antibodies.

2.9. Tube formation assay

ODMECs were suspended in a complete EGM-2MV medium and cultured on matrigel (BD Biosciences, San Jose, CA, USA). After 48

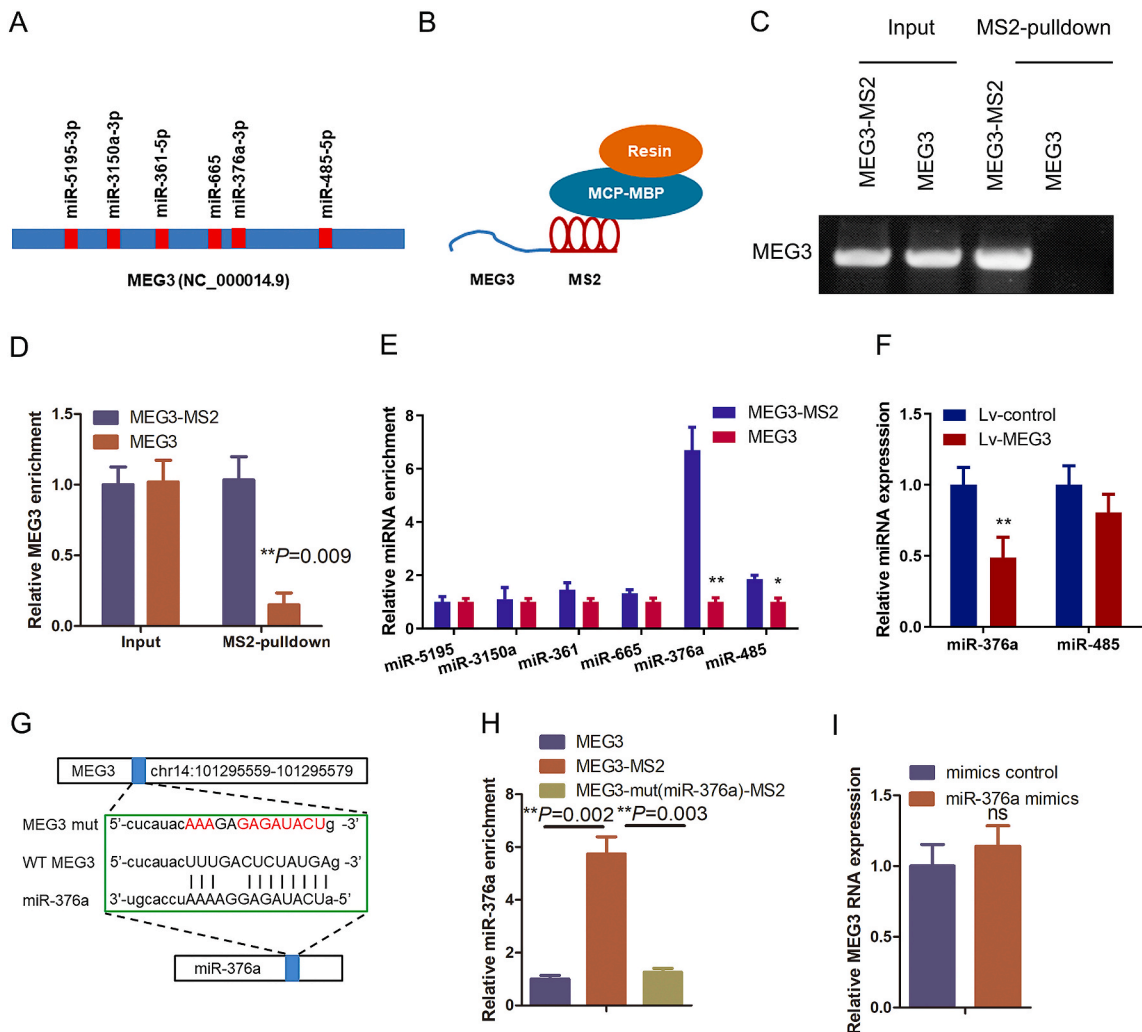


Fig. 2. MEG3 sponges miR-376a. (A) Schematic plotting of binding sites for predicted miRNAs on MEG3. (B) Schematic of the MEG3 conjugate recombinant fusion protein that recognizes the MS2 hairpins. (C) Agarose gel electrophoresis indicated that MBP-MCP–conjugated amylose resin could be used to pull down MEG3. (D) Quantified data of MEG3 enrichment by qRT-PCR. (E) Six different miRNAs were detected by qRT-PCR among the precipitates pulled down with MEG3. (F) miR-376a and miR-485-5p expression were detected by qRT-PCR in Lv-control and Lv-MEG3 letivirus infected ODMECs. (G) Schematic representation of the MEG3-binding sequence in the 3'-UTR of miR-376a. A mutated sequence was generated in the wild-type miR-376a-binding sequence as indicated. (H) miR-376a enrichment levels in ODMECs transfected with MEG3, MEG3-MS2, and MEG3 Mut (miR-376a)-MS2. (I) Steady-state levels of MEG3 in ODMECs transfected with miR-376a mimics. The full, not adjusted blot image for Fig. 2C was included as supplementary materials.

h of incubation, ODMEC tube formation was observed under a Nikon Eclipse microscope and photographed. Tube formation was quantified using different parameters based on counting branching points and cell clusters.

2.10. Statistical analysis

Data were plotted as mean ± standard deviation (SD). At least three biological repeats were performed-the statistical analysis. Differences between two groups were performed using a student's t-test (two-tailed). One-way analysis of variance (ANOVA) with Tukey's posttest was assessed to evaluate data among more than two groups. GraphPad PRISM (version 9, La Jolla, CA, USA) was used in this study and $p < 0.05$ was considered statistically significant.

3. Results

3.1. Downregulation of MEG3 and its inhibitory role in tube formation in ovarian cancer

To explore the roles of MEG3 in ovarian cancer progression, we first quantified the transcript levels of MEG3 with the GEPIA database. MEG3 expression was significantly lower in ovarian cancer tissues than in normal controls (Fig. 1A, supplementary materials). Furthermore, to investigate the correlation of MEG3 to the overall survival rate in patients with ovarian cancer, we divided the

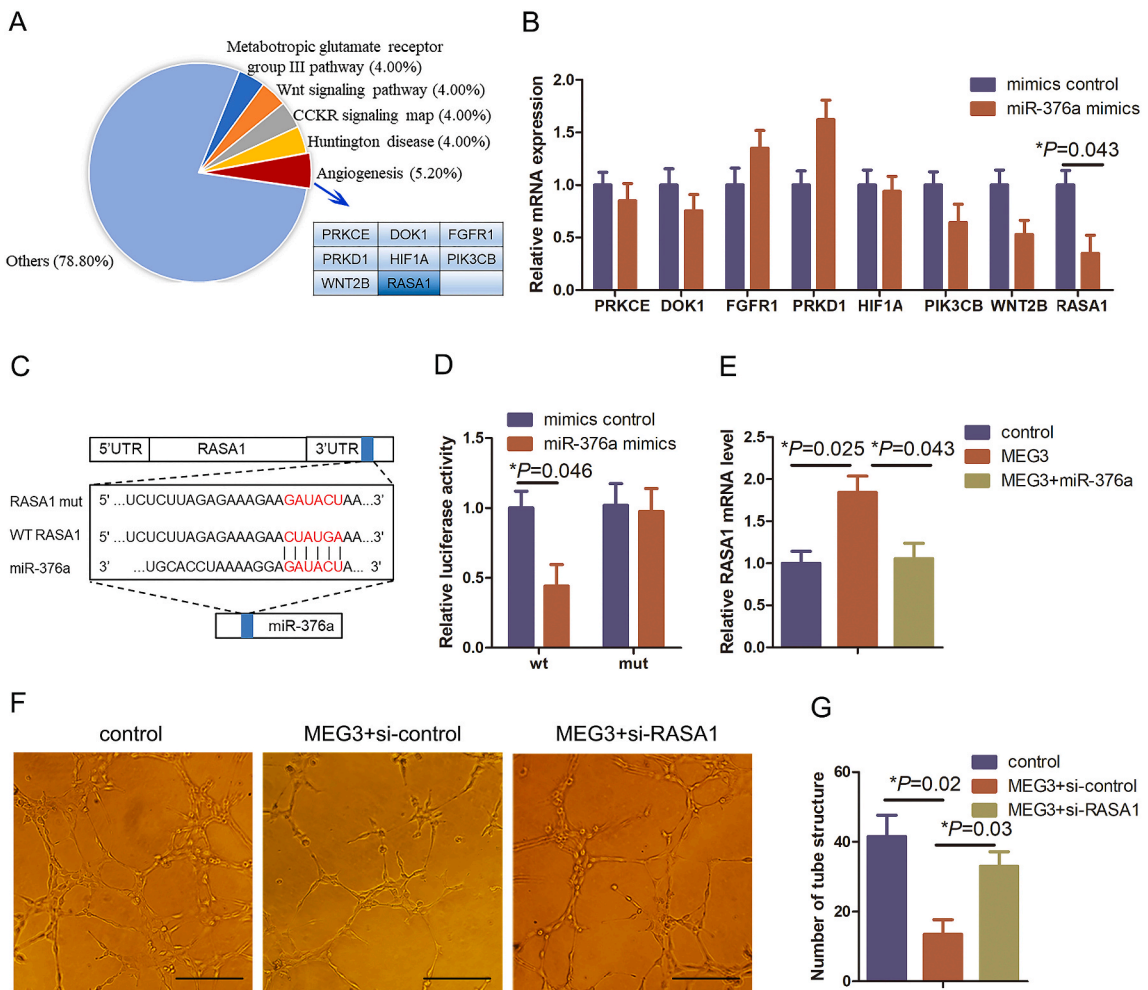


Fig. 3. MEG3/miR-376a loop regulates tube formation. (A) TargetScan prediction genes were collected from the online prediction website. Predicted candidate genes were then analyzed according to the PANTHER classification system. The listed genes are associated with the process of angiogenesis. (B) qRT-PCR analysis depicting the changes in angiogenesis-related genes in ODMECs treated with control mimics and miR-376a mimics. (C) Prediction of miR-376a target sequences in the 3'-UTR of the RASA1 gene and its mutant. (D) Luciferase assay after co-transfection of ODMECs with the wild-type or mutant RASA1 reporter and miR-376a mimics or the control mimics. (E) qRT-PCR analysis of RASA1 expression in ODMECs treated with MEG3 or miR-376a mimics. (F) Tube formation by ODMECs treated with MEG3, si-control, or si-RASA1. Scale bar = 100 μm. (G) Quantified data from F.

samples into two groups (high and low MEG3 levels) based on the mean value of MEG3 expression data. Our analysis showed that high expression of MEG3 was correlated to a high overall survival rate (Fig. 1B). This indicates the role of MEG3 as a tumor suppressor in the context of ovarian cancer.

Since microvascular endothelial cells are the main cellular component responsible for ovarian cancer angiogenesis, the levels and activities of MEG3 in ODMECs were explored. Quantitative analysis showed that MEG3 level was lower in ODMECs than in controls (Fig. 1C), consistent with MEG3 being considered a tumor suppressor for ovarian cancer. To determine the effect of MEG3 in angiogenesis, lentiviral vectors were used to stably restore the expression of MEG3 in ovarian tumor endothelial cells, followed by the examination of tube formation, an assay to quantify the potential of angiogenesis in vitro. Using qRT-PCR, we first confirmed the increase in MEG3 expression (Fig. 1D). The subsequent tube formation assay displayed that increased MEG3 expression inhibited the tube formation in ODMECs (Fig. 1E and F). These results proved that MEG3 restrained tube formation of ODMECs, suggesting the inhibitory role of MEG3 in ovarian cancer angiogenesis.

3.2. MEG3 acts as a platform to sponge miR-376a

MEG3, as a long noncoding RNA, could play important roles in cancer via crosstalk with other RNA species, such as miRNAs. To explore the miRNAs directly interacting with MEG3, a prediction software from Starbase was used to identify miRNA-binding sites on MEG3 RNA. We found MEG3 sequence complementary to six miRNA seed sequences, including miR-5195-3p, miR-3150a-3p, miR-361-5p, miR-665, miR-376a, and miR-485-5p (Fig. 2A). To prove the binding of these six miRNAs to MEG3, MS2 pulldown assays were done on lysates of ODMECs expressing MEG3-MS2 or MEG3 (Fig. 2B–D). The bound miRNAs would be precipitated by MEG3-MS2 and then confirmed by qRT-PCR. Among the six miRNAs predicted from bioinformatics analysis, only miR-376a and miR-485 were shown to be significantly enriched in the precipitates, of which miR-376a reached about five folds increase in MS2 samples compared to negative control samples (Fig. 2E). However, only miR-376a was significantly reduced by miR-376a in ODMECs (Fig. 2F).

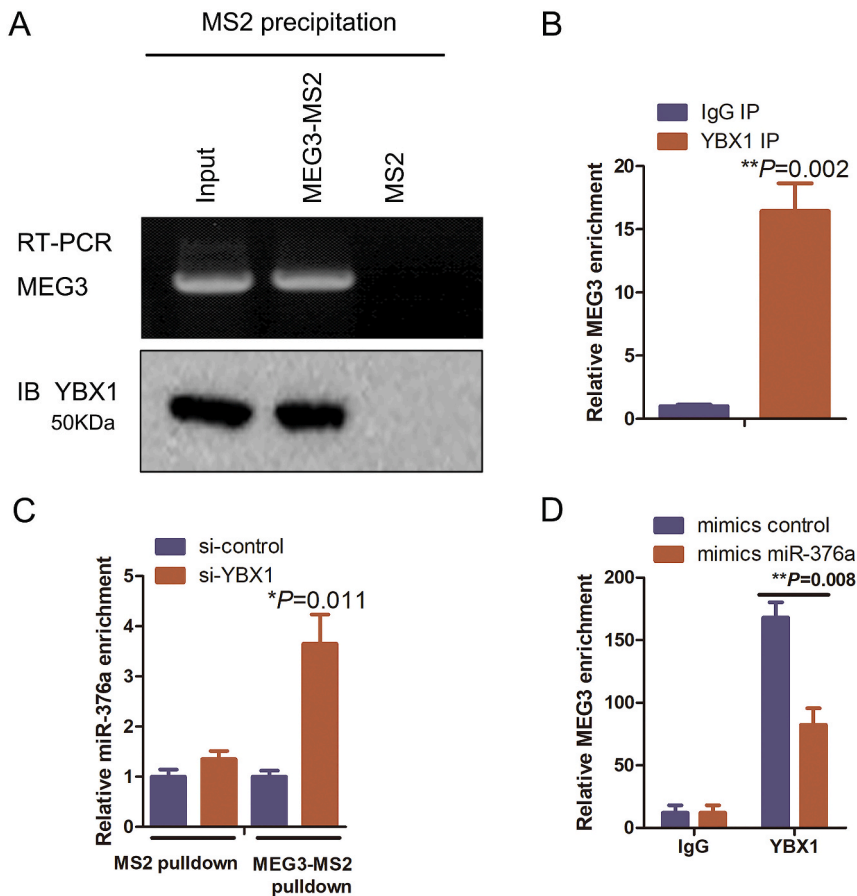


Fig. 4. Competitive binding of YBX1 and miR-376a to MEG3. (A) YBX1 co-precipitated with MEG3. The MEG3-MS2-pulldown assay was performed. Western blot analysis of YBX1 present in the MEG3-MS2 precipitates. (B) RIP analysis of YBX1 interaction with MEG3 in ODMECs. Following YBX1 IP or control using IgG IP, MEG3 levels were quantified by qRT-PCR. (C) MEG3 RNA expression in ODMECs transfected with si-control or si-YBX1. (D) RIP analysis and qRT-PCR detection of MEG3 enrichment in ODMECs treated with mimics control and miR-376a mimics. The full, not adjusted blot images for Fig. 4A and Western blot quantification analysis were included as supplementary materials.

Therefore, the interaction between miR-376a and MEG3 became the focus of our study.

To further assess the sequence responsible for the interaction between MEG3 and miR-376a, we introduced a mutation in the putative miR-376a/MEG3 binding site (Fig. 2G). MEG3-mut-MS2 (with miR-376a binding site mutation) failed to precipitate miR-376a, suggesting that MEG3 directly binds with miR-376a through a complementary sequence (Fig. 2H). Notably, overexpression of miR-376a did not change the MEG3 level (Fig. 2I), suggesting that, instead of being negatively regulated by miR-376a, MEG3 acts as a platform to sponge miR-376a.

3.3. MEG3 suppresses angiogenesis through the miR-376a/RASA1 axis in ODMECs

To understand how MEG3–miR-376a interaction affects angiogenesis, we explored the potential targets of miR-376a via TargetScan. All candidate genes were analyzed by the online web classification PANTHER. It showed that 5.2% of the enriched genes (8 candidate genes) were clustered in the angiogenesis pathway (Fig. 3A). With qRT-PCR, we found that RASA1 was significantly downregulated in ODMECs with miR-376a overexpression (Fig. 3B). Therefore, RASA1, an essential gene in tube formation for angiogenesis, became the top candidate.

To confirm whether miR-376a directly binds to RASA1, we predicted the binding site between the two (Fig. 3C). We next constructed the vectors containing the RASA1 3'-UTR in wild-type or mutant formats followed by firefly luciferase reporter. These vectors were used for co-transfection with miR-376a or control mimics. The reporter assay demonstrated that the expression of miR-376a, instead of control mimics, downregulated the luciferase activity of wild-type RASA1 3'-UTR but not the mutant form (Fig. 3D), which confirmed the direct binding of miR-376a to RASA1.

Based on the above results that MEG3 sponges miR-376a and miR-376a binds to RASA1, we hypothesize that MEG3 suppresses angiogenesis through the miR-376a/RASA1 axis in ODMECs. qRT-PCR analyses showed that overexpression of MEG3 upregulated RASA1. Overexpression of miR-376a simultaneously abrogated MEG3's upregulation on RASA1 (Fig. 3E). This suggested that MEG3 upregulated RASA1 expression, possibly through the abrogation of the binding of miR376a to RASA1 in the process of MEG3's sponging miR-376a. Furthermore, the knockdown of RASA1 abrogated the MEG3-induced suppression of tube formation of ODMECs (Fig. 3F and G). These results suggest that MEG3 regulated tube formation through the miR-376a/RASA1 axis in ODMECs.

3.4. miR-376a and YBX1 compete with each other in binding to MEG3

Recent studies indicated that lncRNAs partner with RBPs to enable certain functions [6]. YBX1, a multi-functional RNA-binding protein, has demonstrated that it can interact with lncRNAs and affect angiogenesis [18]. The interaction between MEG3 with YBX1

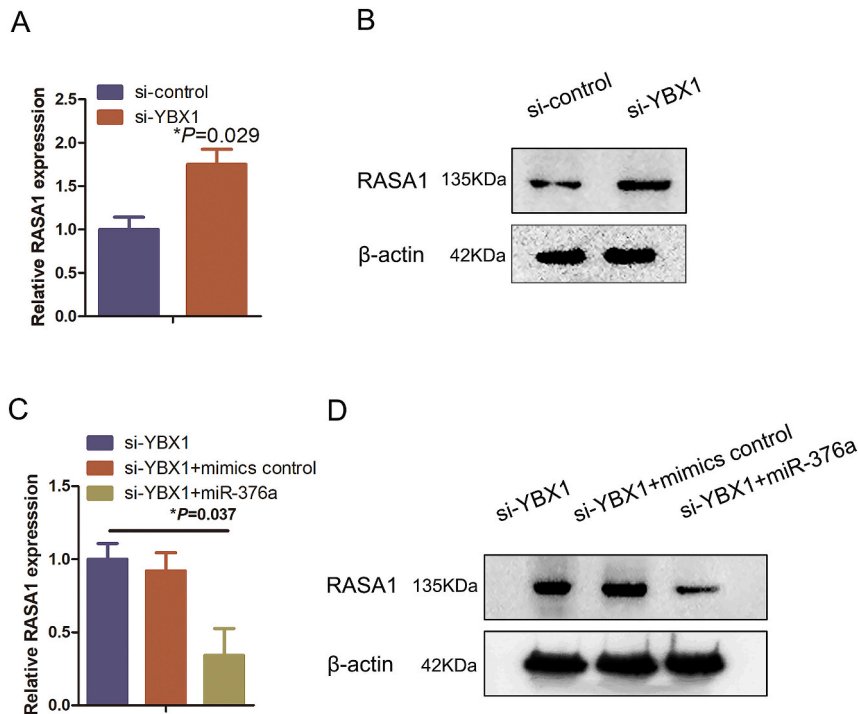


Fig. 5. YBX1 and miR-376a competitively bind to MEG3. (A, B) mRNA level (A) and protein level (B) of RASA1 in ODMECs transfected with si-control or si-YBX1. (C, D) RASA1 mRNA expression (C) and protein level (D) in si-YBX1 transfected ODMECs treated with control or miR-376a mimics. The full, not adjusted blot images (for Fig. 5B and D) and Western blot quantification analysis were included as supplementary materials.

was confirmed by MS2 pulldown assay (Fig. 4A). We then validated the interaction between YBX1 and MEG3 by RIP analysis using anti-YBX1 antibodies and negative control IgG antibodies (Fig. 4B). MEG3 expression was highly enriched in YBX1 IP samples (Fig. 4B), revealing that YBX1 is physically associated with MEG3.

Having demonstrated the binding of miR-376a and YBX1 to MEG3, we explored whether miR-376a and YBX1 competed their binding to MEG3. The MS2 pulldown assay demonstrated that miR-376a was increasingly enriched onto MEG3 when YBX1 was knocked down in ODMECs (Fig. 4C), suggesting a competitive relationship between miR-376a and YBX1 in binding to MEG3. To validate whether the binding of miR-376a to MEG3 affected the binding of YBX1 to MEG3, we used RIP analysis with anti-YBX1 antibodies. In line with the competitive binding hypothesis, compared with mimics control, miR-376a mimics decreased the enrichment of MEG3 association with YBX1 in ODMECs (Fig. 4D). Together these data suggest that YBX1 and miR-376a competitively bind to MEG3.

3.5. Competitive binding network miR-376a/YBX1-MEG3 regulates RASA1 expression

Our results showed that miR-376a is directly bound to RASA1 to downregulate its expression, while miR-376a and YBX1 are competitively bound to MEG3. It would be interesting to investigate whether YBX1 regulated the expression of RASA1. We found that YBX1 knockdown increased the levels of RASA1 from both mRNA and protein aspects (Fig. 5A and B), indicating more miR-376a could be sponged by MEG3, thus leading to the increased level of RASA1. In addition, miR-376a mimics disrupted the increase of mRNA and protein levels of RASA1 in the si-YBX1 condition (Fig. 5C and D). This further sustains the notion that YBX1 and miR-376a competitively bind to MEG3 with each other and regulate the expression of RASA1. Together, these results indicate that MEG3 could sponge miR-376a and regulate the expression of RASA1. We further predicted that YBX1 is bound to MEG3 through a conserved prediction motif. Our results reveal that the YBX1 and miR-376a competitively bind to MEG3, regulate the expression of RASA1, and ultimately affect the tube formation of ODMECs.

4. Discussion

Here we first explored the effects and involved mechanism for MEG3 in ovarian cancer angiogenesis, with ODMECs as in vitro model system. MEG3 was downregulated in ODMECs from our bioinformatics analysis. Overexpression of MEG3 reduced tube formation of ODMECs. Furthermore, MEG3 inhibited tube formation of ODMECs by sponging miR-376a. RASA1, a key angiogenesis suppressor, was directly targeted by miR-376a. YBX1 and miR-376a were competitively bound to MEG3 and regulated the expression of RASA1 (Fig. 6). Our results demonstrated the novel mechanism that MEG3 sponged YBX1 and miR-376a to regulate ovarian cancer angiogenesis through RASA1.

MEG3 was previously shown to promote tube formation in endothelial cells from the umbilical vein and brain, etc. [19–21]. Besides, MEG3 functioned as a tumor suppressor through sponging molecular mechanisms for RBPs or miRNAs in a competing

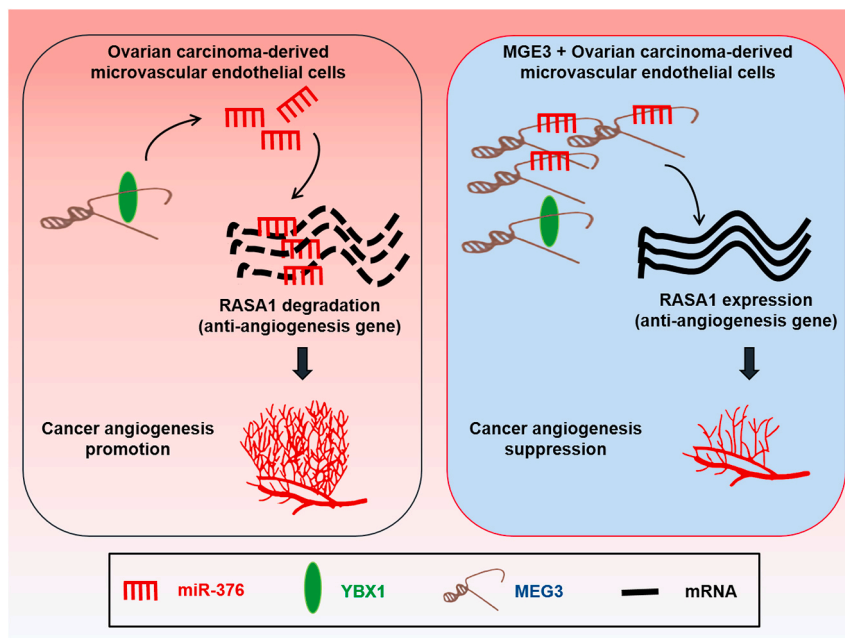


Fig. 6. A model depicting the roles of MEG3 was found to inhibit tube formation of ODMECs by sponging miR-376a. RASA1, a key angiogenesis suppressor, was identified as a direct target gene of miR-376a. YBX1 and miR-376a competitively bind to MEG3 and regulate the expression of RASA1.

endogenous RNA manner. For instance, MEG3 increased TXNIP expression by binding miR-18a in lung tissues, thereby suppressing NLRP3 inflammasome and caspase-1 signaling [22]. In bile acids metabolism, MEG3 destabilized Shp by serving as a guide RNA scaffold to recruit the RBP PTBP1 to Shp mRNA and caused cholestasis [23]. Here, MEG3 sponged both miR-376a and YBX1 to modulate the expression of RASA1, further affecting the tube formation in ODMECs.

We found that miR-376a directly targeted RASA1. RASA1 was reported to function as a suppressor of angiogenesis and played a critical role in the tumorigenicity of hepatocellular carcinoma [24] and capillary malformation-arteriovenous malformation [25]. RASA1 suppresses tube formation in human umbilical vein endothelial cells (HUVECs) via a miRNA-mediated mechanism [26]. In the present study, MEG3 sponged miR-376a and increased RASA1, leading to the suppression of tube formation in ODMECs. miR-376a rescued the effects of MEG3 overexpression on tube formation in ODMECs. These results indicate that MEG3 suppresses tube formation via miR-376a/RASA1 axis. miR-376a expression increased in breast cancer patients' plasma [27] and in pancreatic cancer [28]. In ovarian cancer patients, miR-376a was found at increased levels, and its expression correlated with FIGO stages III-IV [29]. In addition, miR-376a enhanced the proliferation and metastasis of ovarian cancer [30], suggesting that miR-376a could serve as a diagnostic and prognostic biomarker in ovarian cancer. In addition to these oncogenic roles of miR-376a, several studies found that miR-376a could be a tumor suppressor gene [31]. The roles of miRNAs in the context of cancer could be complicated and worth further investigation. Our study enriches the limited knowledge of the roles of miR-376a in ovarian cancer progression.

Our findings reveal that the platform where MEG3 sponges miR-376a and YBX1 play an essential role in ovarian cancer angiogenesis. MEG3 could sponge miR-376a and increase RASA1 expression, suppressing the tube formation of ODMECs. However, binding of YBX1 to MEG3 could release miR-376a from MEG3 and inhibit RASA1 expression, promoting tube formation of ODMECs. This insight provides further clues into how lncRNAs, miRNAs, and RBPs act in coordination to regulate ovarian cancer angiogenesis.

Author contribution statement

Yize Li: Performed the experiments; Analyzed and interpreted the data; Contributed reagents, materials, analysis tools or data.

Lingling Zhang: Performed the experiments; Analyzed and interpreted the data.

Yongmei Zhao: Performed the experiments; Contributed reagents, materials, analysis tools or data.

Hongyan Peng: Contributed reagents, materials, analysis tools or data.

Nan Zhang: Conceived and designed the experiments; Analyzed and interpreted the data; Contributed reagents, materials, analysis tools or data.

Wendong Bai: Conceived and designed the experiments; Analyzed and interpreted the data; Wrote the paper.

Funding statement

Yize Li and Prof. Wendong Bai were supported by National Natural Science Foundation of China [81702554 & 81802661].

Data availability statement

Data included in article/supp. material/referenced in article.

Declaration of interest's statement

The authors declare that they have no known competing financial interests or personal relationships that could have appeared to influence the work reported in this paper.

Appendix A. Supplementary data

Supplementary data related to this article can be found at <https://doi.org/10.1016/j.heliyon.2023.e13204>.

References

- [1] V. Kocbek, S. Imboden, K. Nirgianakis, M. Mueller, B. McKinnon, Dual influence of TNF α on diverse *in vitro* models of ovarian cancer subtypes, *Heliyon* 7 (2) (2021), e06099.
- [2] M. Medeiros, A.O. Ribeiro, L.A. Lupi, G.R. Romualdo, D. Pinhal, L.G.A. Chuffa, F.K. Delella, Mimicking the tumor microenvironment: fibroblasts reduce miR-29b expression and increase the motility of ovarian cancer cells in a co-culture model, *Biochem. Biophys. Res. Commun.* 516 (1) (2019) 96–101.
- [3] J. Li, J. Bai, N. Tuerdi, K. Liu, Long noncoding RNA MEG3 promotes tumor necrosis factor- α induced oxidative stress and apoptosis in interstitial cells of cajal via targeting the microRNA-21/I-kappa-B-kinase beta axis, *Bioengineered* 13 (4) (2022) 8676–8688.
- [4] F. Amini, M. Khalaj-Kondori, A. Moqadami, A. Rajabi, Expression of HOTAIR and MEG3 are negatively associated with *H. pylori* positive status in gastric cancer patients, *Genes Cancer* 13 (2022) 1–8.
- [5] K.F. Meza-Sosa, R. Miao, F. Navarro, Z. Zhang, Y. Zhang, J.J. Hu, C.C.R. Hartford, X.L. Li, G. Pedraza-Alva, L. Pérez-Martínez, A. Lal, H. Wu, J. Lieberman, SPARCLE, a p53-induced lncRNA, controls apoptosis after genotoxic stress by promoting PARP-1 cleavage, *Mol. Cell* 82 (4) (2022), 802.e10-785.e10.
- [6] W. Xu, J. Biswas, R.H. Singer, M. Rosbash, Targeted RNA editing: novel tools to study post-transcriptional regulation, *Mol. Cell* 82 (2) (2022) 389–403.

- [7] D. Wang, Y. Xu, L. Feng, P. Yin, S.S. Song, F. Wu, P. Yan, Z. Liang, RGS5 decreases the proliferation of human ovarian carcinoma-derived primary endothelial cells through the MAPK/ERK signaling pathway in hypoxia, *Oncol. Rep.* 41 (1) (2019) 165–177.
- [8] Z. Tang, C. Li, B. Kang, G. Gao, C. Li, Z. Zhang, GEPIA: a web server for cancer and normal gene expression profiling and interactive analyses, *Nucleic Acids Res.* 45 (W1) (2017). W98–W102.
- [9] B. Györfy, A. Lanczky, A.C. Eklund, C. Denkert, J. Budczies, Q. Li, Z. Szallasi, An online survival analysis tool to rapidly assess the effect of 22,277 genes on breast cancer prognosis using microarray data of 1,809 patients, *Breast Cancer Res. Treat.* 123 (3) (2010) 725–731.
- [10] V. Agarwal, G.W. Bell, J.W. Nam, D.P. Bartel, Predicting effective microRNA target sites in mammalian mRNAs, *Elife* 4 (2015), e05005.
- [11] J.H. Li, S. Liu, H. Zhou, L.H. Qu, J.H. Yang, starBase v2.0: decoding miRNA-ceRNA, miRNA-ncRNA and protein-RNA interaction networks from large-scale CLIP-Seq data, *Nucleic Acids Res.* 42 (Database issue) (2014) D92–D97.
- [12] I. Paz, I. Kosti, M. Ares Jr., M. Cline, Y. Mandel-Gutfreund, RBPmap: a web server for mapping binding sites of RNA-binding proteins, *Nucleic Acids Res.* 42 (Web Server issue) (2014) W361–W367.
- [13] X. Zhang, Y. Zhou, S. Chen, W. Li, W. Chen, W. Gu, LncRNA MACC1-AS1 sponges multiple miRNAs and RNA-binding protein PTBP1, *Oncogenesis* 8 (12) (2019) 73.
- [14] H. Xia, X.L. Qu, L.Y. Liu, D.H. Qian, H.Y. Jing, LncRNA MEG3 promotes the sensitivity of vincristine by inhibiting autophagy in lung cancer chemotherapy, *Eur. Rev. Med. Pharmacol. Sci.* 22 (4) (2018) 1020–1027.
- [15] H. Yan, J. Rao, J. Yuan, L. Gao, W. Huang, L. Zhao, J. Ren, Long noncoding RNA MEG3 functions as a competing endogenous RNA to regulate ischemic neuronal death by targeting miR-21/PDCD4 signaling pathway, *Cell Death Dis.* 8 (12) (2017) 3211.
- [16] A. Uboveja, Y.K. Satija, F. Siraj, D. Saluja, p73-regulated FER1L4 lncRNA sponges the oncogenic potential of miR-1273g-3p and aids in the suppression of colorectal cancer metastasis, *iScience* 25 (2) (2022), 103811.
- [17] O. Lautier, A. Penzo, J.O. Rouvière, G. Chevreux, L. Collet, I. Loïdouce, A. Taddei, F. Devaux, M.A. Collart, B. Palancade, Co-translational assembly and localized translation of nucleoporins in nuclear pore complex biogenesis, *Mol. Cell* 81 (11) (2021) 2417–2427.e5.
- [18] X. Kong, J. Li, Y. Li, W. Duan, Q. Qi, T. Wang, Q. Yang, L. Du, H. Mao, C. Wang, A novel long noncoding RNA AC073352.1 promotes metastasis and angiogenesis via interacting with YBX1 in breast cancer, *Cell Death Dis.* 12 (7) (2021) 670.
- [19] C. Chen, Y. Huang, P. Xia, F. Zhang, L. Li, E. Wang, Q. Guo, Z. Ye, Long noncoding RNA Meg3 mediates ferroptosis induced by oxygen and glucose deprivation combined with hyperglycemia in rat brain microvascular endothelial cells, through modulating the p53/GPX4 axis, *Eur. J. Histochem.* 65 (3) (2021) 3224.
- [20] Y. Jiang, H. Zhu, H. Chen, Y.C. Yu, Y.T. Xu, F. Liu, S.N. He, M. Sagnelli, Y.M. Zhu, Q. Luo, Elevated expression of lncRNA MEG3 induces endothelial dysfunction on HUVECs of IVF born offspring via epigenetic regulation, *Front. Cardiovasc. Med.* 8 (2022), 717729.
- [21] R. Zhan, K. Xu, J. Pan, Q. Xu, S. Xu, J. Shen, Long noncoding RNA MEG3 mediated angiogenesis after cerebral infarction through regulating p53/NOX4 axis, *Biochem. Biophys. Res. Commun.* 490 (3) (2017) 700–706.
- [22] D.M. Zou, S.M. Zhou, L.H. Li, J.L. Zhou, Z.M. Tang, S.H. Wang, Knockdown of long noncoding RNAs of maternally expressed 3 alleviates hyperoxia-induced lung injury via inhibiting thioredoxin-interacting protein-mediated pyroptosis by binding to miR-18a, *Am. J. Pathol.* 190 (5) (2020) 994–1005.
- [23] L. Zhang, Z. Yang, J. Trottier, O. Barbier, L. Wang, Long noncoding RNA MEG3 induces cholestatic liver injury by interaction with PTBP1 to facilitate shp mRNA decay, *Hepatology* 65 (2) (2017) 604–615.
- [24] Y.L. Chen, W.C. Huang, H.L. Yao, P.M. Chen, P.Y. Lin, F.Y. Feng, P.Y. Chu, Down-regulation of RASA1 is associated with poor prognosis in human hepatocellular carcinoma, *Anticancer Res.* 37 (2) (2017) 781–785.
- [25] D. Chen, E.D. Hughes, T.L. Saunders, J. Wu, M.N.H. Vasquez, T. Makinen, P.D. King, Angiogenesis depends upon EPHB4-mediated export of collagen IV from vascular endothelial cells, *JCI Insight* 7 (4) (2022), e156928.
- [26] L. Jing, H. Li, T. Zhang, J. Lu, L. Zhong, MicroRNA-4530 suppresses cell proliferation and induces apoptosis by targeting RASA1 in human umbilical vein endothelial cells, *Mol. Med. Rep.* 19 (5) (2019) 3393–3402.
- [27] K. Cuk, M. Zucknick, D. Madhavan, S. Schott, M. Golatta, J. Heil, F. Marmé, A. Turchinovich, P. Sinn, C. Sohn, H. Junkermann, A. Schneeweiss, B. Burwinkel, Plasma microRNA panel for minimally invasive detection of breast cancer, *PLoS One* 8 (10) (2013), e76729.
- [28] E.J. Lee, Y. Gusev, J. Jiang, G.J. Nuovo, M.R. Lerner, W.L. Frankel, D.L. Morgan, R.G. Postier, D.J. Brackett, T.D. Schmittgen, Expression profiling identifies microRNA signature in pancreatic cancer, *Int. J. Cancer* 120 (5) (2007) 1046–1054.
- [29] X. Meng, S.A. Joosse, V. Müller, F. Trillsch, K. Milde-Langosch, S. Mahner, M. Geffken, K. Pantel, H. Schwarzenbach, Diagnostic and prognostic potential of serum miR-7, miR-16, miR-25, miR-93, miR-182, miR-376a and miR-429 in ovarian cancer patients, *Br. J. Cancer* 113 (9) (2015) 1358–1366.
- [30] L. Yang, Q.M. Wei, X.W. Zhang, Q. Sheng, X.T. Yan, MiR-376a promotion of proliferation and metastases in ovarian cancer: potential role as a biomarker, *Life Sci.* 173 (2017) 62–67.
- [31] X.R. Fan, Z.Y. Zhang, R.H. Wang, Y. Li, Q.Z. Mao, MiR-376a functions as tumor suppressor by targeting SGK3 in renal cell carcinoma, *Eur. Rev. Med. Pharmacol. Sci.* 23 (9) (2019) 3726–3732.